

Simplified and representative bacterial community of maize roots

Ben Niu^a, Joseph Nathaniel Paulson^{b,c}, Xiaoqi Zheng^{b,d}, and Roberto Kolter^{a,1}

^aDepartment of Microbiology and Immunobiology, Harvard Medical School, Boston, MA 02115; ^bDepartment of Biostatistics and Computational Biology, Dana-Farber Cancer Institute, Boston, MA 02115; ^cDepartment of Biostatistics, Harvard T. H. Chan School of Public Health, Boston, MA 02115; and ^dDepartment of Mathematics, Shanghai Normal University, Shanghai 200234, China

Edited by Steven E. Lindow, University of California, Berkeley, CA, and approved February 9, 2017 (received for review September 28, 2016)

Plant-associated microbes are important for the growth and health of their hosts. As a result of numerous prior studies, we know that host genotypes and abiotic factors influence the composition of plant microbiomes. However, the high complexity of these communities challenges detailed studies to define experimentally the mechanisms underlying the dynamics of community assembly and the beneficial effects of such microbiomes on plant hosts. In this work, from the distinctive microbiota assembled by maize roots, through host-mediated selection, we obtained a greatly simplified synthetic bacterial community consisting of seven strains (*Enterobacter cloacae*, *Stenotrophomonas maltophilia*, *Ochrobactrum pilosum*, *Herbaspirillum frisingense*, *Pseudomonas putida*, *Curtobacterium pusillum*, and *Chryseobacterium indologenes*) representing three of the four most dominant phyla found in maize roots. By using a selective culture-dependent method to track the abundance of each strain, we investigated the role that each plays in community assembly on roots of axenic maize seedlings. Only the removal of *E. cloacae* led to the complete loss of the community, and *C. pusillum* took over. This result suggests that *E. cloacae* plays the role of keystone species in this model ecosystem. *In planta* and *in vitro*, this model community inhibited the phytopathogenic fungus *Fusarium verticillioides*, indicating a clear benefit to the host. Thus, combined with the selective culture-dependent quantification method, our synthetic seven-species community representing the root microbiome has the potential to serve as a useful system to explore how bacterial interspecies interactions affect root microbiome assembly and to dissect the beneficial effects of the root microbiota on hosts under laboratory conditions in the future.

maize | synthetic community | community assembly | biological control

Plants and animals grow, die, and, importantly, evolve surrounded by myriad microbes. It is thus not surprising that research from recent years has identified complex, yet stable and predictable, microbial communities associated with specific sites on and within numerous plants (1–13) and animals (14–18). Rapid improvements in DNA sequencing technologies and data analyses have led to an explosion of data describing the microbial communities associated with a growing number of plant and animal species. From studies performed to date, much has been learned about the microbial communities' species composition and dynamics (5, 10, 12, 17, 19). However, in great part, due to the large number of species, ranging from hundreds to thousands, usually found in natural microbial communities associated with plants and animals, we still know relatively little regarding the properties of these host-associated communities (20–23). One approach to overcome the challenges in analyzing the features of communities is to establish simpler host-associated communities under the controlled conditions of the laboratory (2, 5, 24–26).

A simpler host-microbial community system can be obtained by starting with a germ-free host that is then inoculated with a well-defined microbial community. Several such gnotobiotic model systems have been established and have been used in the study of how representative, yet simplified, communities interact with model hosts (2, 5, 24–26). For example, simplified bacterial communities

from the human gut were successfully established in germ-free mice and used to gain insights into how such communities are affected by diet (24). The leaves of the model plant *Arabidopsis thaliana* were inoculated with a simplified bacterial community to characterize how several plant genes shaped the phyllosphere microbiota (26). A synthetic community containing 38 bacterial strains was used to evaluate the abilities of *A. thaliana* mutants with altered immune systems to sculpt the root microbiome (2). In addition, colonization of *Arabidopsis* roots and leaves using a collection of several hundred bacterial isolates showed that the isolates formed assemblies resembling the natural microbiota on their cognate plant locations (5).

Maize (*Zea mays*) is a representative monocotyledon and a crop plant of great significance in food production. Several studies have analyzed the composition of the maize-associated microbial communities. Results from such studies have shown that the composition of the maize rhizosphere microbiota is greatly influenced by host genetics (27–29), soil physicochemical properties (28), and addition of different types of fertilizer (28). Quite importantly, the bacterial communities of the rhizosphere surrounding maize roots were shown to be substantially different from the adjacent bulk soil in terms of bacterial richness, diversity, and relative abundance of taxa (13, 27, 29–32). In addition, on the maize rhizoplane, a significant reduction of microbial diversity relative to the bulk soil was observed (33). These results clearly indicate that maize plants greatly shape the bacterial community composition in their immediate vicinity.

Significance

Many species of microbes colonize plants as members of complex communities. The high complexity of such plant microbial communities poses great difficulty for any experimental analyses aimed at understanding the principles underlying such microbe-plant interactions. In this work, we assembled a greatly simplified, yet representative, synthetic bacterial model community that allowed us to study the community assembly dynamics and function on axenic maize seedlings. This model community interfered with the growth of a plant pathogenic fungus, thus protecting the plant. This model system will prove to be a useful system for future research on plant-microbe interactions.

Author contributions: B.N. and R.K. designed research; B.N. performed research; B.N., J.N.P., and X.Z. analyzed data; and B.N. and R.K. wrote the paper.

The authors declare no conflict of interest.

This article is a PNAS Direct Submission.

Data deposition: The next-generation sequencing data of the 16S rRNA gene survey reported in this paper have been deposited in the Genbank database (BioProject ID no. PRJNA343280, accession nos. SRR4253152–SRR4253209). The complete genome sequences of the seven strains of the simplified synthetic community reported in this paper have been deposited in the GenBank database (BioProject ID no. PRJNA357031, accession nos. CP018756, CP018779–CP018786, CP018845, and CP018846). The Sanger sequencing data have been deposited in the Genbank database (accession nos. KX817243–KX817271 and KX817273–KX817279).

¹To whom correspondence should be addressed. Email: roberto_kolter@hms.harvard.edu.

This article contains supporting information online at www.pnas.org/lookup/suppl/doi:10.1073/pnas.1616148114/-DCSupplemental.

In this work, we chose maize as a model plant to serve as a host to develop a simplified root-associated bacterial community. We grew germ-free maize seedlings in soil and did two selective iterations to arrive at a greatly simplified model bacterial community containing seven bacterial strains: *Enterobacter cloacae*, *Stenotrophomonas maltophilia*, *Ochrobactrum pilosum*, *Herbaspirillum frisingense*, *Pseudomonas putida*, *Curtobacterium pusillum*, and *Chryseobacterium indologenes*. This simplified community reproducibly assembled on the root surfaces. We were able to follow the dynamics of root colonization by a culture-dependent method based on agar plates selective for each of the seven species. By removing one strain at a time, we were able to probe the role played by each species in community assembly. We found that only the removal of *E. cloacae* caused dramatic changes of the community compositions. This finding suggests that *E. cloacae* might play a key role in maintaining the other strains on the roots. We also found that this seven-species community protects maize from colonization by *Fusarium verticillioides* (formerly *Fusarium moniliforme*), the causative agent of seedling blight disease (34–36).

There is precedent for the use of synthetic communities to study plant–microbe interactions. However, these studies have been largely focused on *Arabidopsis* and have used a large number of strains. For example, a synthetic community of 38 strains was useful in demonstrating the importance of salicylic acid in shaping the root-associated microbiota (2). In another study, a mixture of hundreds of isolates was used to show an overlap in the microbiota of leaves and roots (5). One study did use a greatly simplified community of seven strains, rationally selected from known plant-associated microbes, to analyze the effects of *Arabidopsis* genes on the structure of leaf-associated microbial communities (26). The present study is distinct from prior work in several ways. This work was done using maize as the host plant; the model community assembles on roots, and its seven members were chosen, in part, based on the microbes that the host selected on its root. In addition, the absolute abundance of each member can be accurately and relatively easily tracked by growth on selective media. Finally, whereas prior studies have focused on the effects stemming from the plant, this work focuses on characterizing the potential interspecies interactions among the members of this model community and its beneficial effects on hosts. Thus, this simplified community may serve as a useful system to gain insights into the principles behind community assembly and beneficial effects of plant microbiotas.

Results

Maize Roots Assemble a Distinctive Microbiota. To guide our efforts to establish a simplified maize root bacterial community, we

sought guidance from prior studies that analyzed the species composition of plant-associated microbial communities. It is well established that plant hosts exert a strong selection such that root-associated communities are clearly different from those communities found in the rhizosphere and bulk soils (20, 37). This conclusion was shown in seminal early studies using the model plant *Arabidopsis* (1, 2, 4, 38). Furthermore, it was shown that such host selection was driven, in part, by the plant immune signaling in *Arabidopsis* (2). Subsequently, clear differences between the root microbiome and the microbiome of surrounding soils have also been reported in studies on wheat, tomato, cucumber, rice, barley, sugarcane, and eastern cottonwood by using culture-independent analyses (7, 9, 10, 33, 39, 40). Members of four bacterial phyla, Proteobacteria, Firmicutes, Bacteroidetes, and Actinobacteria, make up most of the bacterial diversity of the root microbiota (1, 4, 5, 9, 20, 38, 39, 41–43). However, the structure of the root microbiota at lower taxonomic levels, (e.g., genus) varies depending on the specific host and environmental factors (1, 2, 4, 5, 10, 38).

As a first step toward defining a simple bacterial community that assembles reproducibly and stably on maize roots, we set out to repeat in our laboratory the characterization of the microbial communities formed in roots grown in natural soil. We did so by sequencing the V4 region of the 16S rRNA gene using the Illumina MiSeq platform (44, 45). We designed our approach to be similar to previously reported studies on *Arabidopsis* (1, 4) and collected samples from three compartments (roots, rhizosphere, and bulk soil) (Fig. S1A). In summary, we obtained a total of 778,601 high-quality reads, and the read count per sample ranged from 32,411–68,917, with a median of 41,781 (Dataset S1). After the removal of the plant-derived and low-abundance operational taxonomic units (OTUs), the high-quality reads were clustered into 3,211 OTUs using ≥97% sequence identity as the cutoff (Dataset S2).

Our results were consistent with prior studies done with maize, where host selection was shown to result in clear differences between the community compositions of roots (33) or the rhizosphere (13, 27, 29–32) and the community compositions of soils (Fig. S2 A and B). We observed 13 phyla of relatively high abundance (defined as having an average relative abundance greater than 0.3% in any one sample) and 17 low-abundance phyla (all combined into a single color) (Fig. 1). Importantly, as has been found in previous studies (1, 4, 5, 9, 20, 33, 38, 39, 41–43), four phyla dominated the maize root microbiota (accounting for 95.3% of the total): Proteobacteria (84.4%), Firmicutes (4.3%), Bacteroidetes (3.5%), and Actinobacteria (3.1%). Among these four phyla, Proteobacteria were significantly enriched in maize roots, which is in accordance with early results (33), and Bacteroidetes were enriched in the rhizosphere (Fig. 1, Fig. S3A, and Datasets

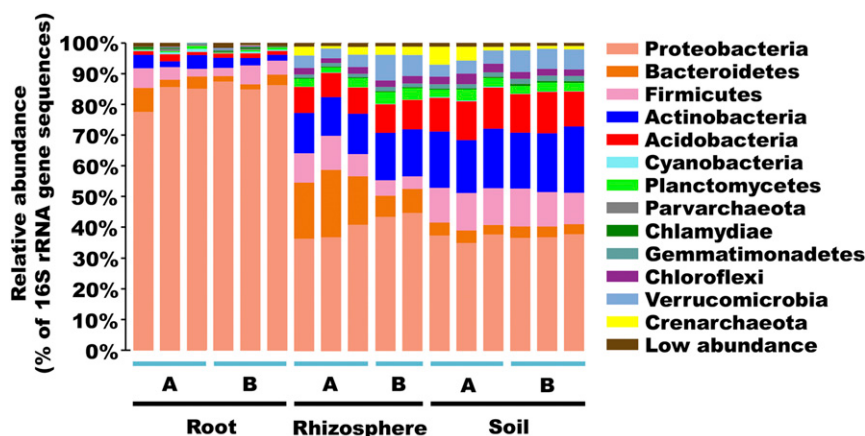


Fig. 1. Histogram of phyla abundances. "A and B" represent bulk soil samples where plants were grown.

S3 and **S4**). At the genus level, *Burkholderia*, *Herbaspirillum*, *Curvibacter*, *Acinetobacter*, Enterobacteriaceae, *Stenotrophomonas*, and *Pseudomonas* (all being Proteobacteria) and *Curtobacterium* (a member of the Actinobacteria) were significantly enriched in the roots (Fig. S3B and Datasets S5 and S6). Our results clearly show that the root enrichment of Proteobacteria was built on the gathering of specific genera, which indicates that maize seedlings establish root-inhabiting bacterial communities by selecting a limited number of genera. This finding suggested the possibility of assembling a representative, yet simplified, bacterial synthetic community from the pool of dominant genera by root selection.

Assembly and Characterization of Simplified Bacterial Communities on Maize Roots. Our second step toward defining a simplified maize root community was to obtain inocula that contained fewer bacterial strains than bulk soil but was still representative of the overall root bacterial microbiota. To this end, we surface-sterilized seeds, germinated them, and grew them for 1 wk in soil. The roots of the resulting seedlings were crushed in PBS buffer, and the released bacteria were used as our starting material for two parallel strategies, I and II (Fig. 2A). In the first strategy (I), we used the root tissue suspension to inoculate surface-sterilized seeds, and the resulting seedlings were grown in sterile 1/2 Murashige and Skoog (MS) agar [0.8% (wt/vol)] (adjusting the pH to 6.0 to simulate the pH of soil A shown in Dataset S7) for 7 d. Bacteria were then released from the seedling roots by washing after sonication. Bacterial dilutions were then plated on 0.1× trypticase soy agar (TSA) plates to obtain single colonies. We sequenced the 16S rRNA genes from 61 independent colonies, and these genes fell into 16 different species (Dataset S8A). Fourteen species were from the phylum Proteobacteria, and the other two were *C. indologenes* and *C. pusillum*, which are members of the Bacteroidetes and Actinobacteria phyla, respectively. The 14 Proteobacteria isolates contained two species from each of the genera *Ochrobactrum* and *Herbaspirillum*; we selected a single species from each: *O. pituitosum* and *H. frisingense*. Four of the Proteobacteria isolates were members of the genus *Enterobacter*; we chose two of these isolates (*E. cloacae* and *E. asburiae*) because a prior publication described them as endophytes of sweet corn roots (46). We were then left with 12 strains (Dataset S8B). We mixed equal volumes of $\sim 10^8$ cells per milliliter suspensions of each species and used the mixture to inoculate 10 seedlings. In our second strategy (II), rather than inoculating the root tissue suspension onto seedlings, we plated dilutions of it directly onto 0.1× TSA plates to obtain isolated colonies. We selected colonies displaying diverse morphologies and determined their 16S rRNA gene sequences. From these colonies, we selected 33 isolates. All of the 33 isolates belonged to four phyla, Proteobacteria, Firmicutes, Bacteroidetes, and Actinobacteria. These isolates, together with two isolates from strategy I (*Dyella* sp. and *C. pusillum*) plus three well-studied rhizobacterial strains [*Bacillus amyloliquefaciens* FZB42 (47), *Paenibacillus polymyxa* M-1 (48), and *Azospirillum brasiliense* sp7 (49)], made up a consortium of 38 strains (Dataset S8C). Equal volumes of an $\sim 10^8$ cells per milliliter suspension of each of these 38 strains were mixed, and the mixture was used to inoculate six axenic seedlings.

After 5 d of growth, we determined the community compositions present on each of the 16 seedlings' roots (10 from strategy I and six from strategy II) by determining the 16S rRNA gene sequences present and analyzing the results using the Quantitative Insights into Microbial Ecology (QIIME) (50) and cluster-free filter (CFF) (51) approaches (Fig. 2A and Datasets S9 and S10). Despite the large differences in the inoculum compositions, both strategies yielded rather similar simplified root-associated communities.

From both strategies, members of the genus *Enterobacter* dominated the communities (Fig. 2A and Dataset S9). From strategy I, the input strains *S. maltophilia*, *O. pituitosum*, *H. frisingense*, *P. putida*, *C. pusillum*, and *C. indologenes* were all present at least at

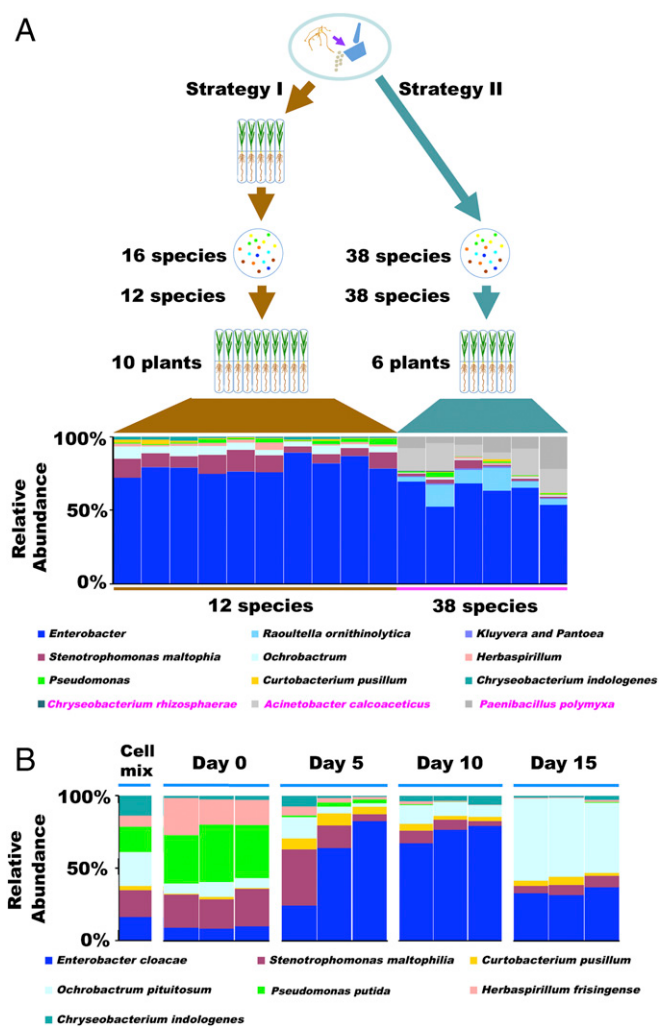


Fig. 2. Simplified bacterial model community of maize roots was obtained by host-mediated selection. (A) Two strategies were used for isolating bacteria that could colonize root surfaces for 5 d. *A. calcoaceticus* and *P. polymyxa* were included in the 38 species for inoculation in strategy II, but were not involved in strategy I. In both strategies, the structure profiles of the bacterial community were measured by 16S rRNA gene sequencing and using QIIME combined with CFF for sequence data analysis. The relative abundances of *Kluyvera* and *Pantoea*, which possess an identical sequence for the V4 region of the 16S rRNA genes, are summed as "Kluyvera and Pantoea." Three species, *Chryseobacterium rhizospherae*, *A. calcoaceticus*, and *P. polymyxa*, only used in the 38-species inoculum for strategy II are colored pink. (B) Dynamics of the seven-strain bacterial community on the maize root surface were tracked from day 0 immediately after inoculation for 15 d by using 16S rRNA gene sequencing. The "Cell mix" represents the seven species mixed and used as the inoculum. The y axis is relative abundance calculated as percentages of 16S rRNA gene sequences.

a 1.0% average relative abundance. In contrast, the input strains *Kluyvera* sp. and *Pantoea septica* were present at a very low average relative abundance (<0.3%). *Raoultella ornithinolytica* was nearly not detected, whereas *Dyella* sp. was undetectable. Surprisingly, even though the inoculum from strategy II was much more complex, the resulting communities were very similar. In all roots, *Enterobacter* was the most dominant taxon. *S. maltophilia*, *O. pituitosum*, *H. frisingense*, *P. putida*, *C. pusillum*, and *C. indologenes* were also all present. In addition, two species that were not involved in the inoculum of strategy I, *Paenibacillus polymyxa* and *Acinetobacter calcoaceticus*, were detected in the plants from strategy II. In summary, there were seven strains common to both

strategies: *E. cloacae*, *S. maltophilia*, *O. pituitosum*, *H. frisingense*, *P. putida*, *C. pusillum*, and *C. indologenes* [In previous experiments, we had used four different species of *Enterobacter* in the two strategies. Because prior publications indicated that *E. cloacae* was a good maize root colonizer (46, 52), we chose to include only that species in all subsequent experiments.]

From the above results we derived a list of seven species to mix and use as inocula for further testing of community assemblage. They are *E. cloacae*, *S. maltophilia*, *O. pituitosum*, *H. frisingense*, *P. putida*, *C. pusillum*, and *C. indologenes*. Using a mixture of these seven species, we inoculated axenic seedlings and followed the microbial community dynamics on the roots over 15 d (Fig. 2B and Datasets S11 and S12). Although the relative abundance of each of the seven strains varied over the duration of our experiments, all seven were still present even after 15 d. Quite importantly, the results varied little from plant to plant. Thus, we were able to construct a highly simplified bacterial community that reproducibly assembles on the roots of maize seedlings (Fig. 2B). Clearly, this seven-strain community is by no means the only combination possible. Indeed, given that we had input multiple strains from several different genera in some cases, the question remained as to whether using strains from different species of the same genus would have an observable effect on community dynamics. We did test a seven-strain combination with a different species of *Enterobacter* (*E. asburiae*) and obtained very similar results (Fig. S44 and Dataset S13). In addition, we tested one nine-strain combination where we replaced *O. pituitosum* with *Ochrobactrum otisci* and added *P. polymyxa* and *A. calcoaceticus*. In this case, the relative amounts of the seven genera used for the experiments shown in Fig. 2B were still very similar (Fig. S44 and Dataset S13). Thus, for the rest of the experiments presented here, we used the same seven-strain community used in the experiments shown in Fig. 2B. Interestingly, the seven species present in the simplified community we used are all members of the dominant genera of the maize root microbiota (Fig. S3B and C). This result suggests that this synthetic community may be representative of the root microbiota. To test this idea further, we analyzed our microbiome sequencing data to determine if OTUs representing each of the seven species were originally present in the roots. Indeed, we found representative OTUs present in the roots of maize seedlings (Fig. S4B and C and Dataset S14). Anticipating that these seven strains may become widely used by other researchers, we wanted to perform some initial characterization of each one. To this end, we sequenced their genomes and deposited the sequences in the National Center for Biotechnology Information database.

This seven-species synthetic community that assembles on maize roots can serve as a useful system for investigating the dynamics of root colonization, characterizing the underlying interspecies interactions, and defining the role that each member plays in the community. Such studies require that the abundance of each species can be easily, quickly, and accurately quantified. Although next-generation sequencing (NGS)-based (culture-independent) methods to obtain species abundance are useful (26, 44), they generally have three limitations: (i) a relatively long turnaround time (it may take up to a week from DNA extraction until the acquisition and final analyses of sequencing data), (ii) they are not particularly well-suited to determining the absolute abundance of each species in the community accurately, and (iii) interference of host DNA and bias introduced by PCR amplification. Recently, some alternative techniques have been applied independently or together with NGS to reduce the processing time (26, 53), determine the absolute abundance of bacteria from a given phylum (2, 54), and eliminate the interference of host DNA and PCR bias (55), but it is still not easy to use one single existing approach to overcome or bypass the three limitations simultaneously, which prompted us to seek a more efficient solution. Given the simplicity of our model community and the culturability of all of its members, we decided to develop a

culture-dependent, simple, rapid, and economical method to assess the abundance of each member of the community.

Development of a Culture-Dependent Method for Quantifying Community Composition

The main challenge to the establishment of a culture-dependent approach for quantifying the abundance of each species and the composition of the seven-species simplified community is how to distinguish each species from the others by culturing. As a first step to achieve this goal, we used the phenotype microarray (PM) technology (56). We evaluated 288 unique culture conditions related to the chemical sensitivity and the osmotic response with each of the seven bacterial strains (Figs. S5A and B and Dataset S15). From these studies, we obtained seven different conditions that selectively permitted only the growth of each individual strain (Table S1). For each strain, the recovery efficiency under the selective condition was very close to 1 (Table S1). The compositions of the mixed cell suspensions and the structure of the model community on maize roots were assessed by both colony-forming unit (cfu) counting and 16S rRNA gene sequencing. Both methods yielded very similar average relative abundances, and the compositions of the cell mix suspensions determined by the two methods were highly similar to the “expected” ratio; the composition determined by cfu counting showed an especially significant positive correlation ($r = 0.8818$, $P = 0.0091$) to the expected ratio. Also, the structure of the model community on maize roots determined by the two methods was very similar. The structure determined by 16S rRNA gene sequencing and normalized by the ribosomal RNA operon number of each species was significantly positively correlated to the structure determined by cfu counting ($r = 0.9643$, $P = 0.0014$) (Fig. 3 and Dataset S16). Similar results were obtained in a second independent experiment (Fig. S5C and Dataset S16). These results indicate that the culture-dependent method we developed can be used to determine the composition of the seven-species community on maize roots accurately. In previous studies, the quantification of plant synthetic bacterial communities was mainly performed with culture-independent methods: automated ribosomal intergenic spacer analysis (ARISA) (26, 53) or 16S rRNA gene amplicon sequencing (2, 5). Both methods have been proved to be well suited for accurate determination of the community structure. However, regarding the measurement of the absolute abundance of each species in the communities, ARISA only works in a semi-quantitative way (26, 53), whereas 16S rRNA gene amplicon sequencing needs to be combined with additional technique(s) (e.g., catalyzed reporter deposition-fluorescence in situ hybridization) (54). In this work, our culture-dependent method is low-cost and very fast, and it permits accurate determination of the absolute cfu numbers of each species present on the roots.

Contribution of Each Species to the Ability of the Other Species to Remain Present in the Community. Recently, much has been learned regarding the structure of the microbial communities present on the roots of different plant species (1, 3–7, 9, 10). However, these communities are so complex that our knowledge of how they assemble and what role each species plays in determining community structure is rudimentary at best. The seven-species community that we have defined here represents a much simpler system to carry out analyses on community assembly and the role that individual species play in the process. Not only do we have a simple system but we have also developed conditions that allow us to determine the absolute abundance of each species on the root very quickly.

As a first step toward understanding community assembly, we determined the effect of removing individual species one at a time. We used the seven mixes of six species each (with one of the species from the original seven-member community removed), plus the seven-species mix, to inoculate axenic seedlings and then followed the dynamics of community composition by determining the abundance of each species (by cfu counting). The average

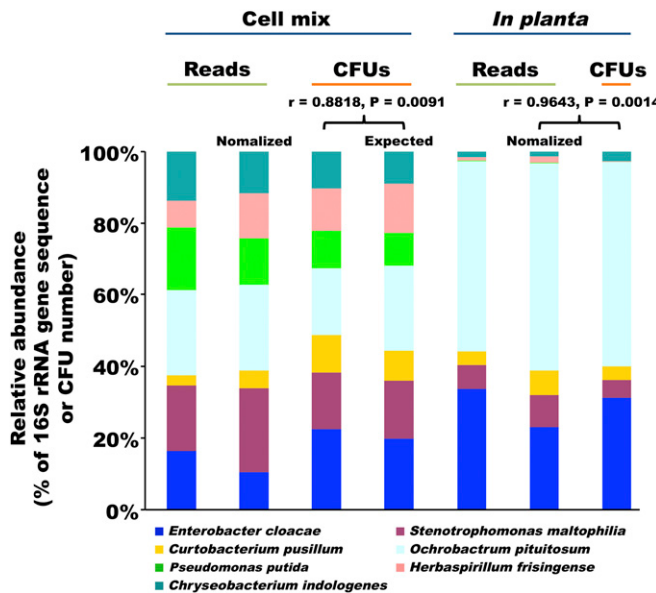


Fig. 3. Comparison of the culture-dependent selective plate method and the culture-independent 16S rRNA gene sequencing method for determining the composition of the seven-species synthetic community. The two methods were applied in parallel to samples of mixed cell suspensions (*Cell mix*) and to 15-d-old maize roots colonized with the seven-strain community labeled as “*In planta*.” The outputs from the 16S rRNA gene sequencing and the culture-dependent method are marked as “Reads” and “CFUs,” respectively. “Normalized” indicates that the results obtained with sequencing were normalized with the ribosomal RNA operon number of each of the seven species, and “Expected” means the supposed compositions of the mixed cell suspensions. The Spearman’s rank correlation coefficients were calculated for cell mix compositions vs. expected ratio, and community structure was determined by 16S rRNA gene sequencing vs. community structure determined by cfu counting.

relative abundances obtained from two independent experiments are displayed as bar charts in Fig. 4 and Fig. S64 (Dataset S17). The different community compositions obtained were clustered based on the Bray–Curtis (BC) dissimilarity index. We also determined the α -diversity of each community by calculating its Shannon index (H) scores. The seven-species community (C7) dynamics parallel the results of a similar experiment already shown in Fig. 2B, reinforcing the conclusion that this community’s assembly and dynamics are reproducible. For six of the seven single-species removal experiments, the overall dynamics are broadly similar to the overall dynamics observed with the seven-species communities (i.e., their H scores remain relatively high along the three sampling times), which suggests these communities keep relatively high evenness. In stark contrast, removal of *E. cloacae* (−Ecl) leads to dramatic changes in community composition and α -diversity. Without *E. cloacae*, the communities quickly became dominated by *C. pusillum*, and by day 15, the other five species were at or near extinction, driving the H scores to near 0 (0.005 ± 0.004). The removal of *P. putida* (−Ppu) also led to an increase in the relative abundance of *C. pusillum*, but its takeover was never as dramatic, and the resulting H scores remained relatively high.

A key control was to determine if the maize seedlings were indeed necessary to yield the dynamics of the community structure we observed and show in Fig. 4 and Fig. S64; the possibility remained that the results were simply due to bacterial interactions in MS agar, irrespective of the plant. To test this possibility, we performed control experiments in the same gnotobiotic system but without maize seedlings. The seven-species mix was inoculated in MS agar; we then followed the dynamics of bacterial community composition for 15 d and found that the compositions of the

communities on maize root and in MS agar are indeed significantly different (Fig. S7 A–C and Datasets S18A and S19A). In addition, when we removed *E. cloacae* and followed the dynamics in MS agar without seedlings, *C. pusillum* did not take over (Fig. S7 D–F and Datasets S18B and S19B). Thus, our key observations indeed depend on the presence of the maize seedlings.

It was not clear whether the changes in the relative abundance of each species, as displayed in Fig. 4, were due to overgrowth of *C. pusillum*, disappearance of the other species, or both. Our culture-dependent assay, where we determine absolute abundances,

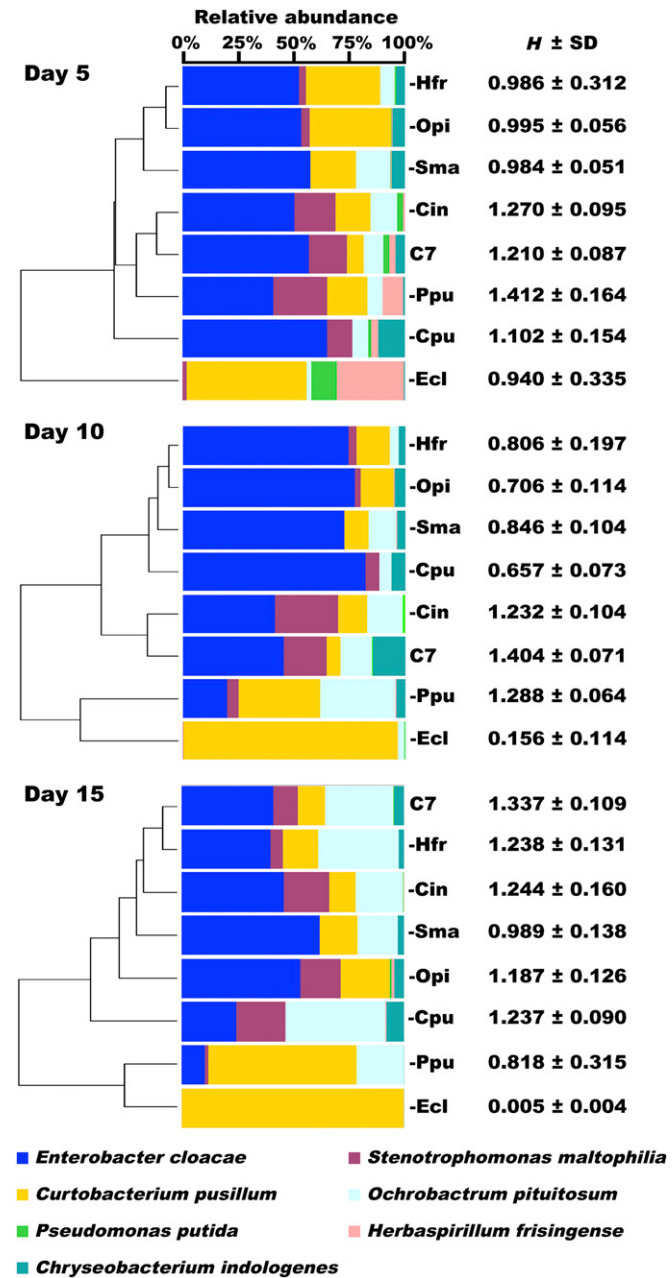


Fig. 4. Clustering analysis of the compositions of the seven-species synthetic community and seven six-species communities along the 15-d growth of maize seedlings. The samples were collected at day 5, day 10, and day 15. −Sma, −Opi, −Cpu, −Ecl, −Cin, −Hfr, and −Ppu represent the six-species communities resulting from the removal of *S. maltophilia*, *O. pituitosum*, *C. pusillum*, *E. cloacae*, *C. indologenes*, *H. frisingense*, and *P. putida*, respectively. The communities are clustered based on the BC dissimilarity index.

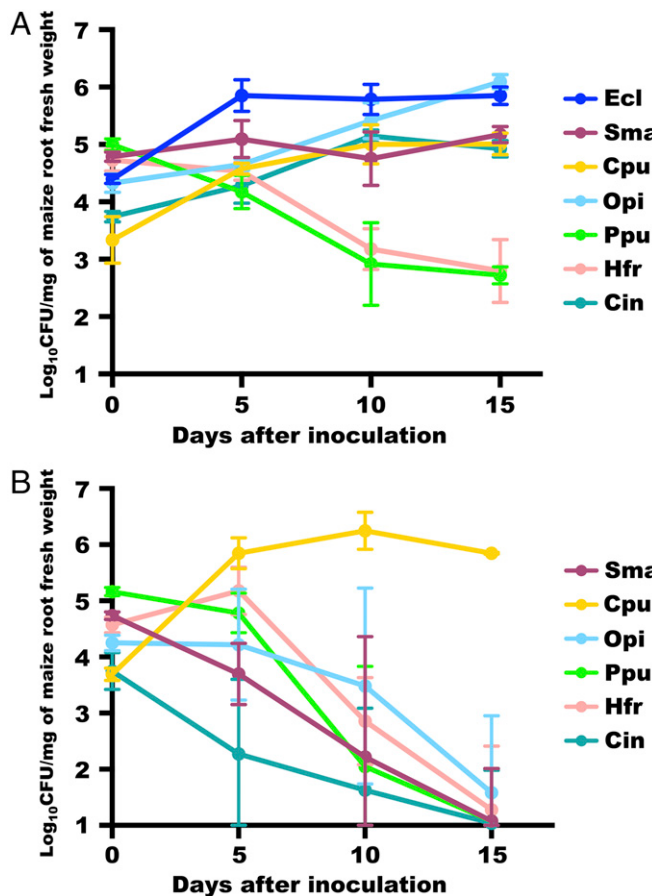


Fig. 5. Growth of each strain in the seven-species synthetic community (A) and the six-species community without *E. cloacae* (B) on maize roots determined by cfu counting.

allowed us to resolve this matter. In Fig. 5 and Fig. S6B (Dataset S20), we plotted the absolute abundances of each species in C7 and the community lacking *E. cloacae* ($-Ecl$) along different sampling times. In C7, the absolute abundances of five species increased after inoculation, whereas *P. putida* and *H. frisingense* decreased in number (Fig. 5A). The growth of *E. cloacae* and *S. maltophilia* reached saturation at day 5, and the abundance of *C. indologenes* reached its maximum at day 10. Afterward, these three species maintained relatively stable levels. In contrast, *O. pituitosum* and *C. pusillum* kept growing during the 15 d of the experiment. The maximum abundances of the five species were $\sim 7.9 \times 10^4$ to 1.3×10^6 cfu/mg (of fresh weight of maize root), up from 2.1×10^3 to 6.1×10^4 cfu/mg on day 0, determined immediately after inoculation. *P. putida* and *H. frisingense* displayed a continuous decline. At day 15, the abundances of these two species dropped to 4.7×10^2 and 6.3×10^2 cfu/mg from 9.9×10^4 cfu/mg and 5.3×10^4 cfu/mg, respectively (Fig. 5A). In contrast, in the $-Ecl$ experiment (Fig. 5B), only the abundances of *C. pusillum* and *H. frisingense* rose after inoculation, whereas the abundances of the other four species dropped sharply from 5.6×10^3 to 1.5×10^5 cfu/mg to less than 1.0×10^2 cfu/mg. *H. frisingense* grew until day 5, when its abundance reached the maximum, and then quickly decreased from $\sim 1.5 \times 10^5$ cfu/mg to less than 1.0×10^2 cfu/mg. *C. pusillum* grew until day 10, and its abundance increased from 4.9×10^3 cfu/mg to 1.8×10^6 cfu/mg and remained at a relative stable level (Fig. 5B). Our results show that the removal of *E. cloacae* caused the decrease of the absolute abundances of *S. maltophilia*, *O. pituitosum*, and *C. indologenes*. Moreover, the abundances of *P. putida* and *H. frisingense* dropped even faster in $-Ecl$ than in C7, whereas the growth of *C. pusillum*

was dramatically stimulated. Thus, the results proved that the community dynamics we observed from Fig. 4 and Fig. S6A resulted from both overgrowth of *C. pusillum* and disappearance of the other species.

To gain a better sense of the reproducibility of the community dynamics, we analyzed the results obtained from each individual plant. To this end, we compared the BC distance between each six-species community and the seven-species model community plant by plant (Fig. 6, Fig. S6C, and Dataset S21). The values of the BC distance between the bacterial community on each seedling inoculated with the mixes of six species and the seven-species model community colonized on each plant at 5, 10, and 15 d postinoculation are plotted in Fig. 6. The data points for each comparison within each plant are, in general, narrowly distributed, and the results are also very similar from plant to plant for the same removal and time point. Thus, in general, these results corroborate the reproducibility of this model system. The majority of data points from the six-species communities (excluding $-Ecl$) represent BC distance values of less than 0.5. This finding indicates that the compositions of the communities inhabiting each individual plant were similar to the composition of C7. Notably, the BC distance values rose strikingly and maintained relatively high values (0.81–0.96) when *E. cloacae* was removed. Also, in $-Ppu$, three plants at day 15 showed relatively high BC distance values (0.76–0.80). The results are consistent with the dendograms shown in Fig. 4, where $-Ppu$ and $-Ecl$ cluster together at day 15. Taken together, our results point at *E. cloacae* as the most important species in the seven-species community in terms of the community's ability to maintain all seven species present at all times. Earlier studies with synthetic bacterial communities showed that plant immune signaling is involved in sculpting the root microbiome (2) and that plant host genetic factors affect the phyllosphere microbiota (26) and the microbiota specialization to their respective cognate host organs (5). Thus, prior studies were mainly focused on the effects of host changes on the community dynamics or assembly. In contrast, in our work with the seven-species community, efforts are primarily placed on revealing the

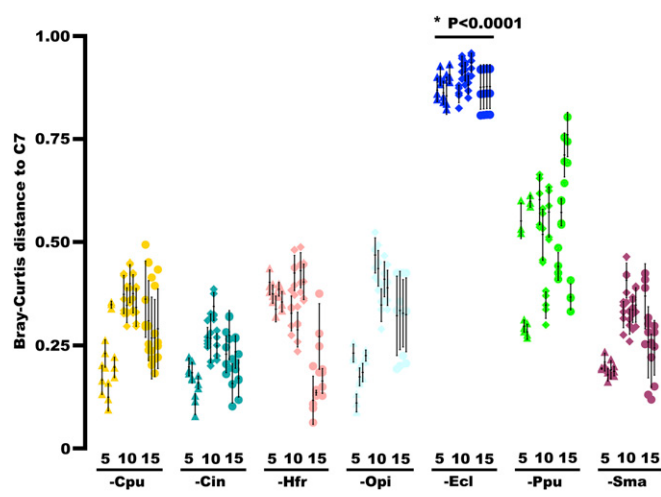


Fig. 6. Comparison of BC distances between each six-species community and the seven-species model community plant by plant. Each dot represents a BC distance value between the bacterial community on one plant colonized by a six-species community and the bacterial community on one plant colonized by the seven-species model community. The asterisk indicates a statistically significant difference ($*P < 0.05$). $-Sma$, $-Opi$, $-Cpu$, $-Ecl$, $-Cin$, $-Hfr$, and $-Ppu$ designate the six-species communities as in Fig. 4. The triangle, square, and circular symbols represent the samples collected at 5 d, 10 d, and 15 d after inoculation, respectively. Fisher's least significant difference (LSD) test was used for the analysis.

role of potential interactions among bacteria in assembling the community on maize roots.

Inhibition Effects of the Model Community Against the Pathogen *F. verticillioides*

***F. verticillioides*.** In addition to studying the model community assembly on maize roots, we evaluated its potential beneficial effects on the host plants. The root microbiota has been demonstrated to contribute to the growth and health of host plants (21). First, we compared the seed germination rate, root fresh weight, and root length of the community-treated plants with those parameters in sterile plants. No significant differences in these parameters were detected between the community-treated and sterile plants (Fig. S8 and Dataset S22). However, we did find effects of the model community when we investigated its interactions with a plant pathogenic fungus.

We examined the inhibitory effect of the community against the fungal pathogen *F. verticillioides*, the cause of maize seedling blight (34–36). Through an *in vivo* fungal colonization assay, we found that the growth of *F. verticillioides* mycelia on the surfaces of the seeds inoculated with the community was significantly delayed compared with the growth on the bacteria-free seeds (Movie S1) and the seeds inoculated with *Escherichia coli* DH5 α (Fig. 7 and Dataset S23A). Two days after inoculation, the fungal mycelia started appearing on the surfaces of seeds treated with *F. verticillioides* and *F. verticillioides* jointly with *E. coli*. The average colonization rates of the two treatments were the same, 13% (Fig. 7A). On the third day after inoculation, mycelia were present on the surfaces of nearly all of the seeds treated with *F. verticillioides* (100%) and *F. verticillioides* jointly with *E. coli* (97%). However, there was no fungal growth visible on the surfaces of seeds inoculated with *F. verticillioides* jointly with the model community until the fourth day after inoculation. At that point, the percentage of seeds colonized by fungi was only 3%, significantly lower than the percentage of the seeds inoculated with *F. verticillioides* (100%)

and *F. verticillioides* jointly with *E. coli* (100%) (Fig. 7A and B). Such delayed growth of *F. verticillioides* lasted until the ninth day postinoculation. At that point, the fungal colonization percentage of the seeds inoculated with *F. verticillioides* jointly with the model community reached 82%. However, this colonization percentage was still significantly lower than the colonization percentage of seeds treated with *F. verticillioides* and *F. verticillioides* jointly with *E. coli* ($P = 0.0303$) (Dataset S23A). On the tenth day postinoculation, the differences between the colonization percentages of the *F. verticillioides* jointly with the model community and the other two became nonsignificant (Fig. 7A).

We also compared the severity of the maize seedling blight of the three treatments. Our results revealed that the seedlings treated with *F. verticillioides* jointly with the model community displayed the lowest disease severity index (Fig. 7C and Dataset S24A; disease ranks are provided in Fig. S9A). Also, much less fungal growth was observed on fungi-colonized seeds of the *F. verticillioides* jointly with community than the fungal growth of the other two treatments (Fig. 7B). In short, this seven-species community is capable of reducing maize seedling blight by delaying the colonization of *F. verticillioides*. This finding suggests the potential of using this community for biological control of the maize seedling blight. We also tested the inhibitory property of the bacterial community against *F. verticillioides* *in vitro* on potato dextrose agar and nutrient agar plates. Our results showed that the community significantly suppressed the growth of *F. verticillioides* on both types of agar plates (Fig. 7D and Dataset S25).

Next, we tested the inhibitory effects of each of the seven species individually against *F. verticillioides*. We found all of the seven species delayed the colonization of *F. verticillioides* and reduced the severity of the seedling blight to varying degrees (Fig. S9B and C and Datasets S23B and S24B). Among the seven species, *E. cloacae* showed the highest efficiency in delaying *F. verticillioides*

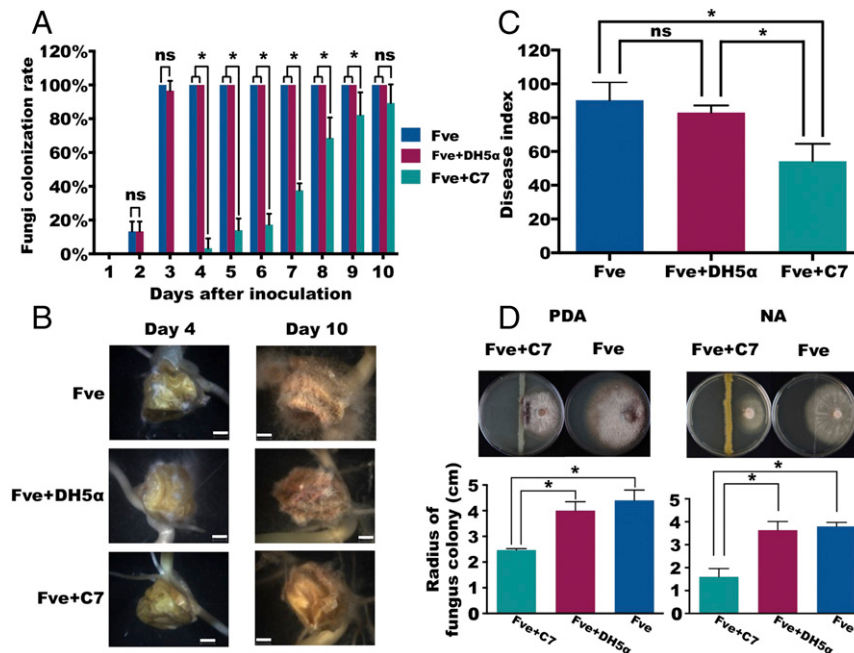


Fig. 7. Antagonistic effect of the seven-species model community against *F. verticillioides*. (A) Delaying effect of the seven-species model community on *F. verticillioides* colonization. (B) Inhibitory effect of the seven-species community on *F. verticillioides* mycelial growth on the surfaces of maize seeds. Photographs were taken on day 4 and day 10 after inoculation. (Scale bars: 2 mm.) (C) Biocontrol effect of the seven-species community against maize seedling blight caused by *F. verticillioides*. (D) Inhibitory effects of the seven-species community on the growth of *F. verticillioides* on potato dextrose agar (PDA) and nutrient agar (NA) plates *in vitro*. Fve, treatment with *F. verticillioides* alone; Fve+C7, joint treatment with *F. verticillioides* and the seven-species model community; Fve+DH5 α , joint treatment with *F. verticillioides* and *E. coli* DH5 α . Asterisks indicate that differences among the means represented by the columns are statistically significant (* $P < 0.05$). ns, nonsignificant difference. Fisher's LSD test was used for the analysis.

colonization. The colonization percentage of seedlings treated with *E. cloacae* was significantly lower than the colonization percentage of seedlings treated with *F. verticillioides* and *F. verticillioides* plus *E. coli* until the sixth day postinoculation, 2 d earlier than the seven-species community treatment (Fig. S9B). Similarly, *E. cloacae* also exhibited the best biocontrol effect against maize seedling blight among the seven members of the community. The average disease severity index of the seedlings treated with *E. cloacae* was around 60, which is significantly lower than the average disease severity index of seedlings treated with *F. verticillioides* and *F. verticillioides* jointly with *E. coli*, but still higher than the average disease severity index of the seven-species community treatment (Fig. S9C and Dataset 24B). Thus, our results indicate that although each one of the seven members of the community showed some biocontrol effects against *F. verticillioides* individually, such effects were not as strong as the biocontrol effects exhibited by the entire community. This finding corroborates the diversity resistance hypothesis (57, 58). The increased resistance to *F. verticillioides* invasion in the community-treated maize seedlings may be due to a high number of species interactions (57) and intensified competition for niche space (59, 60). These *in planta* interactions between the seven-species synthetic community and *F. verticillioides* may prove to be a promising system to investigate the biological control effects of plant microbiotas.

Discussion

That plants selectively recruit microbes from the soil to establish a characteristic yet very complex microbiota on their roots has been demonstrated by numerous studies (1–9, 61, 62). This complexity makes detailed mechanistic studies on how root microbial communities assemble and function challenging, given the tools available today. One possible way to gain insights into the workings of root microbial communities is to establish greatly simplified multispecies communities able to colonize plant roots stably. The results presented in this work provide a robust and representative seven-species community of the maize root microbiota, which reproducibly assembles and persists on the roots of axenic maize seedlings.

Before the development of the seven-species community, we analyzed the microbiota that assembled on the roots of maize seedlings grown in soil. Clearly, the communities that assembled on those roots were very different from the communities found in the rhizosphere and the original soil (Dataset S26). Those results are consistent with earlier findings on other plant species (1, 2, 4, 7, 9, 10, 20, 33, 37–40). In previous studies on the maize microbiome, the remarkable difference between the bacterial community of the rhizosphere (13, 27, 29–32) or rhizoplane (33) and the bacterial community of bulk soil was also demonstrated. Thus, our findings corroborate the knowledge of the niche-mediated plant microbiota structure.

Based on these results, which indicated that the maize seedlings select a subset of species present in bulk soil, we used host-mediated microbiota selection as an aid in obtaining a greatly simplified synthetic community that was representative of the more complex initial communities and able to colonize roots. Such approaches have been recently proposed and applied to improve plant and animal health (63–65). These strategies emphasize the selection of microbial communities indirectly through the host (63). After two rounds of host selection (strategy I in Fig. 24), we obtained a simplified bacterial synthetic community consisting of seven species that were members of the maize root microbiota (Fig. S4B and C). Among the seven strains, *P. putida* is the most abundant in the root microbiome, which is inconsistent with the previous findings that *Pseudomonas* dominated in maize rhizosphere (29, 30, 66) and rhizoplane (33) bacterial communities, where the relative abundance of *Pseudomonas* was up to 67% (33). In addition, *Herbaspirillum*, *Enterobacter*, *Stenotrophomonas*, *Chryseobacterium*, and *Ochrobactrum* were all reported as dominant members of the maize

root-associated microbiota (13, 66), whereas *Curtobacterium* was characterized as an endophyte inhabiting the root of sweet corn (46). Therefore, our host-mediated microbiota selection worked efficiently to capture the dominant members of the maize root microbiome.

By using this approach of letting the host select before isolating individual bacterial species, most noncandidate species were excluded. Another advantage of this selection model is that there is no need to consider large numbers of combinations of candidate bacterial strains, because the plant host selects the community as a whole. Considering that different plant species may share a fair portion of their root microbiota (1, 4, 5, 9, 10, 20, 38, 39, 41–43), a host selection approach might lead to communities that assemble and are maintained in different plant species. The seven-species model bacterial community we have developed is much simpler than the synthetic communities developed using *Arabidopsis* roots (2, 5). However, the seven species are still taxonomically representative of the maize root microbiota (Figs. S3B and C and Fig. S4B and C). Thus, this simplified community should serve as a useful laboratory system to study root assemblages and maize bacterial microbiota interactions in detail. Nonetheless, we acknowledge that it is impossible for this seven-species model community to possess all of the bacterial interactions and functions within the root microbiota. We also notice that the ratio of the seven strains changed significantly in the simplified community compared with their ratios in the root microbiota (Fig. S4C). Similar changes were also observed in a synthetic bacterial community representing the most abundant phyla in the *Arabidopsis* phyllosphere, where the relative abundance of *Rhodococcus* sp. belonging to Actinobacteria was 1% (67, 68) and increased dramatically to 40% in the synthetic community (26), which led to the finding that the distributions of the *Rhodococcus* sp. and other members were less even in the synthetic community than in the phyllosphere microbiome, and that the ratio of Proteobacteria and Actinobacteria decreased to around 1:1 in the defined community (26) from about 15:1 in the phyllosphere microbiota (41). This outcome may be due to the variation in the number of microbial interactions. In the synthetic communities, the absence of so many other microbes may lead to different interaction networks among the synthetic community members, which probably gives rise to the different relative abundances. We believe that our development of a culture-dependent assay to obtain the absolute abundances of individuals from each species quickly and easily makes this model system very attractive. The turnaround time, accuracy, cost, and ease of manipulation make this assay very “user-friendly” compared with nucleic acid sequencing.

One of the key fundamental questions in studies of microbial communities is how multiple species of bacteria coexist and assemble into a community. In natural settings, the assemblage of a bacterial community can be influenced by diverse factors, including the interactions within the community, the hosts, and the spatial distributions of the members. Bacterial interactions (69), host genotypes (2, 26), niche specificities (5), and spatial distributions (70) are key factors for the assemblage of simple synthetic communities. Due to the high complexity of the microbiota in environmental settings such as plant roots, it is difficult to probe the significance of bacterial interactions experimentally. The simplified seven-species bacterial community that establishes on maize roots has allowed us to investigate experimentally the importance of each member to the assemblage of the community. Specifically, we performed colonization assays with all community combinations lacking one species. Among the seven unique mixes lacking one species, only one led to dramatic changes in community composition: When we removed *E. cloacae*, *C. pusillum* took over the population. This result suggests that *E. cloacae* is a key member for assemblage of the community, and is reminiscent of the ecological concept of keystone species (71, 72). From the absolute abundance data we obtained (Fig. 5), we found that the removal of *E. cloacae* led to a sharp decrease in the abundances of

S. maltophilia, *O. pituitosum*, and *C. indologenes*. In contrast, *C. pusillum* grew much more rapidly in the absence of *E. cloacae*. These population dynamics suggest that *E. cloacae* may interact positively with *S. maltophilia*, *O. pituitosum*, and *C. indologenes* and negatively with *C. pusillum*. However, the molecular details of the bacterial interactions within the seven-species community are likely very complex and will be the subject of future studies.

The plant-associated microbiota can serve as a protective barrier against invading pathogens (21, 58, 63). Such beneficial communities are capable of controlling pathogens in both direct and indirect ways (21). Recently, altering the microbiota to protect hosts from pathogens in ways that do not necessarily kill the pathogens have been proposed and applied (73–75). However, because of the high complexity, knowledge of the mechanisms through which the microbiota protects plants from pathogens is very limited. Our greatly simplified synthetic community controlled maize seedling blight caused by *F. verticillioides* (34) through inhibiting fungal colonization (Fig. 7A) and arresting hyphal expansion growth (Fig. 7D) under gnotobiotic conditions in the laboratory. Although we do not yet understand the underlying molecular mechanisms for this biological control, there is hope that the simplicity of the community will make such studies possible in the near future.

1. Lundberg DS, et al. (2012) Defining the core *Arabidopsis thaliana* root microbiome. *Nature* 488(7409):86–90.
2. Lebeis SL, et al. (2015) PLANT MICROBIOME. Salicylic acid modulates colonization of the root microbiome by specific bacterial taxa. *Science* 349(6250):860–864.
3. Wagner MR, et al. (2016) Host genotype and age shape the leaf and root microbiomes of a wild perennial plant. *Nat Commun* 7:12151.
4. Bulgarelli D, et al. (2012) Revealing structure and assembly cues for *Arabidopsis* root-inhabiting bacterial microbiota. *Nature* 488(7409):91–95.
5. Bai Y, et al. (2015) Functional overlap of the *Arabidopsis* leaf and root microbiota. *Nature* 528(7582):364–369.
6. Cardinale M, Grube M, Erlacher A, Quehenberger J, Berg G (2015) Bacterial networks and co-occurrence relationships in the lettuce root microbiota. *Environ Microbiol* 17(1):239–252.
7. de Souza RSC, et al. (2016) Unlocking the bacterial and fungal communities assemblages of sugarcane microbiome. *Sci Rep* 6:28774.
8. Berg G, Smalla K (2009) Plant species and soil type cooperatively shape the structure and function of microbial communities in the rhizosphere. *FEMS Microbiol Ecol* 68(1):1–13.
9. Edwards J, et al. (2015) Structure, variation, and assembly of the root-associated microbiomes of rice. *Proc Natl Acad Sci USA* 112(8):E911–E920.
10. Ofek-Lazar M, et al. (2015) Niche and host-associated functional signatures of the root surface microbiome. *Nat Commun* 5:4950.
11. Beckers B, et al. (2016) Lignin engineering in field-grown poplar trees affects the endosphere bacterial microbiome. *Proc Natl Acad Sci USA* 113(8):2312–2317.
12. Ritpitakphong U, et al. (2016) The microbiome of the leaf surface of *Arabidopsis* protects against a fungal pathogen. *New Phytol* 210(3):1033–1043.
13. Haichar FZ, et al. (2008) Plant host habitat and root exudates shape soil bacterial community structure. *ISME J* 2(12):1221–1230.
14. Okumura R, et al. (2016) Lypd8 promotes the segregation of flagellated microbiota and colonic epithelia. *Nature* 532(7597):117–121.
15. Mark Welch JL, Rossetti BJ, Rieken CW, Dewhurst FE, Borisy GG (2016) Biogeography of a human oral microbiome at the micron scale. *Proc Natl Acad Sci USA* 113(6):E791–E800.
16. Forslund K, et al.; MetaHIT consortium (2015) Disentangling type 2 diabetes and metformin treatment signatures in the human gut microbiota. *Nature* 528(7581):262–266.
17. Oh J, et al.; NISC Comparative Sequencing Program (2014) Biogeography and individuality shape function in the human skin metagenome. *Nature* 514(7520):59–64.
18. Yasuda K, et al. (2015) Biogeography of the intestinal mucosal and luminal microbiome in the rhesus macaque. *Cell Host Microbe* 17(3):385–391.
19. Sunagawa S, et al.; Tara Oceans coordinators (2015) Ocean plankton. Structure and function of the global ocean microbiome. *Science* 348(6237):1261359.
20. Bulgarelli D, Schlaepipi K, Spaepen S, Ver Loren van Themaat E, Schulze-Lefert P (2013) Structure and functions of the bacterial microbiota of plants. *Annu Rev Plant Biol* 64:807–838.
21. Berendsen RL, Pieterse CM, Bakker PA (2012) The rhizosphere microbiome and plant health. *Trends Plant Sci* 17(8):478–486.
22. Kubinak JL, et al. (2015) MyD88 signaling in T cells directs IgA-mediated control of the microbiota to promote health. *Cell Host Microbe* 17(2):153–163.
23. O'Connor RM, et al. (2014) Gill bacteria enable a novel digestive strategy in a wood-feeding mollusk. *Proc Natl Acad Sci USA* 111(47):E5096–E5104.
24. Faith JJ, McNulty NP, Rey FE, Gordon JI (2011) Predicting a human gut microbiota's response to diet in gnotobiotic mice. *Science* 333(6038):101–104.
25. McNulty NP, et al. (2011) The impact of a consortium of fermented milk strains on the gut microbiome of gnotobiotic mice and monozygotic twins. *Sci Transl Med* 3(106):106ra106.
26. Bodenhausen N, Bortfeld-Miller M, Ackermann M, Vorholt JA (2014) A synthetic community approach reveals plant genotypes affecting the phyllosphere microbiota. *PLoS Genet* 10(4):e1004283.
27. Peiffer JA, et al. (2013) Diversity and heritability of the maize rhizosphere microbiome under field conditions. *Proc Natl Acad Sci USA* 110(16):6548–6553.
28. Aira M, Gómez-Brandón M, Lazcano C, Bäth E, Domínguez J (2010) Plant genotype strongly modifies the structure and growth of maize rhizosphere microbial communities. *Soil Biol Biochem* 42(12):2276–2281.
29. Bouffaoud ML, et al. (2012) Is diversification history of maize influencing selection of soil bacteria by roots? *Mol Ecol* 21(1):195–206.
30. García-Salamanca A, et al. (2013) Bacterial diversity in the rhizosphere of maize and the surrounding carbonate-rich bulk soil. *Microb Biotechnol* 6(1):36–44.
31. Gomes N, et al. (2001) Bacterial diversity of the rhizosphere of maize (*Zea mays*) grown in tropical soil studied by temperature gradient gel electrophoresis. *Plant Soil* 232(1–2):167–180.
32. Sanguin H, et al. (2006) Potential of a 16S rRNA-based taxonomic microarray for analyzing the rhizosphere effects of maize on *Agrobacterium* spp. and bacterial communities. *Appl Environ Microbiol* 72(6):4302–4312.
33. Ofek M, Voronov-Goldman M, Hadar Y, Minz D (2014) Host signature effect on plant root-associated microbiomes revealed through analyses of resident vs. active communities. *Environ Microbiol* 16(7):2157–2167.
34. Baldwin TT, et al. (2014) Maize seedling blight induced by *Fusarium verticillioides*: Accumulation of fumonisin B₁ in leaves without colonization of the leaves. *J Agric Food Chem* 62(9):2118–2125.
35. Glenn AE, Gold SE, Bacon CW (2002) *Fdb1* and *Fdb2*, *Fusarium verticillioides* loci necessary for detoxification of preformed antimicrobials from corn. *Mol Plant Microbe Interact* 15(2):91–101.
36. Kommedahl T, Windels CE (1981) *Root-, Stalk-, and Ear-Infecting Fusarium Species on Corn in the USA* (The Pennsylvania State Univ Press, University Park, PA).
37. Reinhold-Hurek B, Bünger W, Burbano CS, Sabale M, Hurek T (2015) Roots shaping their microbiome: Global hotspots for microbial activity. *Annu Rev Phytopathol* 53:403–424.
38. Schlaepipi K, Dombrowski N, Oter RG, Ver Loren van Themaat E, Schulze-Lefert P (2014) Quantitative divergence of the bacterial root microbiota in *Arabidopsis thaliana* relatives. *Proc Natl Acad Sci USA* 111(2):585–592.
39. Bulgarelli D, et al. (2015) Structure and function of the bacterial root microbiota in wild and domesticated barley. *Cell Host Microbe* 17(3):392–403.
40. Gottel NR, et al. (2011) Distinct microbial communities within the endosphere and rhizosphere of *Populus deltoides* roots across contrasting soil types. *Appl Environ Microbiol* 77(17):5934–5944.
41. Bodenhausen N, Horton MW, Bergelson J (2013) Bacterial communities associated with the leaves and the roots of *Arabidopsis thaliana*. *PLoS One* 8(2):e56329.
42. Guttman DS, McHardy AC, Schulze-Lefert P (2014) Microbial genome-enabled insights into plant-microorganism interactions. *Nat Rev Genet* 15(12):797–813.
43. Hacquard S, et al. (2015) Microbiota and host nutrition across plant and animal kingdoms. *Cell Host Microbe* 17(5):603–616.

Materials and Methods

The bacterial microbiota of the maize roots, rhizosphere, and bulk soil was analyzed by sequencing the 16S rRNA gene amplified by PCR from the genomic DNA extracted from the three sample types discussed above under greenhouse conditions. The sequencing was performed on the Illumina MiSeq platform (44, 45) ([Dataset S27](#)). The analysis of sequencing data was carried out with the QIIME (50) pipeline and CFF (51) approaches. The simplified synthetic communities were assembled on the roots of axenic maize seedlings grown in an MS agar-based gnotobiotic system. The selective growth condition for each of the seven strains of the model community was determined with PM technology (56). The dynamics of the compositions of the seven-species model community and the six-species communities (resulting from the removal of each one of the seven species) were followed by cfu counting on selective plates and 16S rRNA gene sequencing. The biological control effects of the seven-species synthetic community against the maize seedling blight disease were evaluated under laboratory conditions. The inhibitory effects of the model community against *F. verticillioides* were also tested. Further details of materials and methodology are provided in [SI Materials and Methods](#).

ACKNOWLEDGMENTS. We thank Koji Yasuda for data analysis; Dr. Charles Bacon for his generous gift of *F. verticillioides* strains; Dr. Scott Chimileski for the imaging analyses of fungal growth inhibition; Dr. Alejandro Reyes and Dr. Meng Wu for valuable advice on data analysis and comments on the manuscript; and Dr. Nicholas Griffin, Dr. Kornelia Smalla, Dr. Ching-Hong Yang, and members of the R.K. laboratory for valuable advice. B.N. was supported, in part, by a China Green Health Agriculture Postdoctoral Fellowship. J.N.P. was supported by NIH Grants 5R01-HL111759 and 1U01-CA190234 (to John Quackenbush). This work was supported by NIH Grant GM58218 (to R.K.).

44. Caporaso JG, et al. (2011) Global patterns of 16S rRNA diversity at a depth of millions of sequences per sample. *Proc Natl Acad Sci USA* 108(Suppl 1):4516–4522.
45. Caporaso JG, et al. (2012) Ultra-high-throughput microbial community analysis on the Illumina HiSeq and MiSeq platforms. *ISME J* 6(8):1621–1624.
46. Mcinroy JA, Kloepper JW (1995) Survey of indigenous bacterial endophytes from cotton and sweet corn. *Plant Soil* 173(2):337–342.
47. Chen XH, et al. (2007) Comparative analysis of the complete genome sequence of the plant growth-promoting bacterium *Bacillus amyloliquefaciens* FZB42. *Nat Biotechnol* 25(9):1007–1014.
48. Niu B, et al. (2013) Polymyxin P is the active principle in suppressing phytopathogenic *Erwinia* spp. by the biocontrol rhizobacterium *Paenibacillus polymyxa* M-1. *BMC Microbiol* 13(1):137.
49. Kumar S, et al. (2012) Bacteriophytocrome controls carotenoid-independent response to photodynamic stress in a non-photosynthetic rhizobacterium, *Azospirillum brasilense* Sp7. *Sci Rep* 2:872.
50. Caporaso JG, et al. (2010) QIIME allows analysis of high-throughput community sequencing data. *Nat Methods* 7(5):335–336.
51. Tikhonov M, Leach RW, Wingreen NS (2015) Interpreting 16S metagenomic data without clustering to achieve sub-OTU resolution. *ISME J* 9(1):68–80.
52. Hinton DM, Bacon CW (1995) *Enterobacter cloacae* is an endophytic symbiont of corn. *Mycopathologia* 129(2):117–125.
53. Ramette A (2009) Quantitative community fingerprinting methods for estimating the abundance of operational taxonomic units in natural microbial communities. *Appl Environ Microbiol* 75(8):2495–2505.
54. Eickhorst T, Tippkötter R (2008) Improved detection of soil microorganisms using fluorescence *in situ* hybridization (FISH) and catalyzed reporter deposition (CARD-FISH). *Soil Biol Biochem* 40(7):1883–1891.
55. Lundberg DS, Yourstone S, Mieczkowski P, Jones CD, Dangl JL (2013) Practical innovations for high-throughput amplicon sequencing. *Nat Methods* 10(10):999–1002.
56. Bochner BR (2009) Global phenotypic characterization of bacteria. *FEMS Microbiol Rev* 33(1):191–205.
57. Case TJ (1990) Invasion resistance arises in strongly interacting species-rich model competition communities. *Proc Natl Acad Sci USA* 87(24):9610–9614.
58. Wei Z, et al. (2015) Trophic network architecture of root-associated bacterial communities determines pathogen invasion and plant health. *Nat Commun* 6:8413.
59. van Elsas JD, et al. (2012) Microbial diversity determines the invasion of soil by a bacterial pathogen. *Proc Natl Acad Sci USA* 109(4):1159–1164.
60. Kennedy TA, et al. (2002) Biodiversity as a barrier to ecological invasion. *Nature* 417(6889):636–638.
61. Inceoglu Ö, Al-Soud WA, Salles JF, Semenov AV, van Elsas JD (2011) Comparative analysis of bacterial communities in a potato field as determined by pyrosequencing. *PLoS One* 6(8):e23321.
62. Hardoin PR, et al. (2011) Rice root-associated bacteria: Insights into community structures across 10 cultivars. *FEMS Microbiol Ecol* 77(1):154–164.
63. Mueller UG, Sachs JL (2015) Engineering microbiomes to improve plant and animal health. *Trends Microbiol* 23(10):606–617.
64. Swenson W, Wilson DS, Elias R (2000) Artificial ecosystem selection. *Proc Natl Acad Sci USA* 97(16):9110–9114.
65. Panke-Buisse K, Poole AC, Goodrich JK, Ley RE, Kao-Kniffin J (2015) Selection on soil microbiomes reveals reproducible impacts on plant function. *ISME J* 9(4):980–989.
66. Chauhan PS, Chaudhry V, Mishra S, Nautiyal CS (2011) Uncultured bacterial diversity in tropical maize (*Zea mays* L.) rhizosphere. *J Basic Microbiol* 51(1):15–32.
67. Vorholt JA (2012) Microbial life in the phyllosphere. *Nat Rev Microbiol* 10(12):828–840.
68. Delmotte N, et al. (2009) Community proteogenomics reveals insights into the physiology of phyllosphere bacteria. *Proc Natl Acad Sci USA* 106(38):16428–16433.
69. Mee MT, Collini JJ, Church GM, Wang HH (2014) Syntrophic exchange in synthetic microbial communities. *Proc Natl Acad Sci USA* 111(20):E2149–E2156.
70. Kim HJ, Boedicker JQ, Choi JW, Ismagilov RF (2008) Defined spatial structure stabilizes a synthetic multispecies bacterial community. *Proc Natl Acad Sci USA* 105(47):18188–18193.
71. Cottree-Jones HEW, Whittaker RJ (2012) Perspective: The keystone species concept: A critical appraisal. *Front Biogeogr* 4(3):117–127.
72. Steele JA, et al. (2011) Marine bacterial, archaeal and protistan association networks reveal ecological linkages. *ISME J* 5(9):1414–1425.
73. Vale PF, et al. (2016) Beyond killing: Can we find new ways to manage infection? *Evol Med Public Health* 2016(1):148–157.
74. Xue C, et al. (2015) Manipulating the banana rhizosphere microbiome for biological control of Panama disease. *Sci Rep* 5:11124.
75. Ventorino V, et al. (2016) Chestnut green waste composting for sustainable forest management: Microbiota dynamics and impact on plant disease control. *J Environ Manage* 166:168–177.
76. Lane DJ (1991) 16S/23S rRNA sequencing. *Nucleic Acid Techniques in Bacterial Systematics*, eds Stackebrandt E, Goodfellow M (Wiley, New York), pp 115–175.
77. Edgar RC (2010) Search and clustering orders of magnitude faster than BLAST. *Bioinformatics* 26(19):2460–2461.
78. Edgar RC, Haas BJ, Clemente JC, Quince C, Knight R (2011) UCHIME improves sensitivity and speed of chimer detection. *Bioinformatics* 27(16):2194–2200.
79. Caporaso JG, et al. (2010) PyNAST: A flexible tool for aligning sequences to a template alignment. *Bioinformatics* 26(2):266–267.
80. Price MN, Dehal PS, Arkin AP (2009) FastTree: Computing large minimum evolution trees with profiles instead of a distance matrix. *Mol Biol Evol* 26(7):1641–1650.
81. Paulson JN, Stine OC, Bravo HC, Pop M (2013) Differential abundance analysis for microbial marker-gene surveys. *Nat Methods* 10(12):1200–1202.
82. Paulson JN, Pop M, Bravo HC (2015) metagenomeSeq: Statistical analysis for sparse high-throughput sequencing. Bioconductor package 1.10.0. Available at ccb.umd.edu/software/metagenomeSeq. Accessed May 15, 2016.
83. van Diepeningen AD, de Vos OJ, Zelenov VV, Semenov AM, van Bruggen AH (2005) DGGE fragments oscillate with or counter to fluctuations in cultivable bacteria along wheat roots. *Microb Ecol* 50(4):506–517.
84. Buddrus-Schiemann K, Schmid M, Schreiner K, Welzl G, Hartmann A (2010) Root colonization by *Pseudomonas* sp. DSMZ 13134 and impact on the indigenous rhizosphere bacterial community of barley. *Microb Ecol* 60(2):381–393.
85. Wilson K (2001) Preparation of genomic DNA from bacteria. *Curr Protoc Mol Biol*, 10.1002/0471142727.mb0204s56.
86. Chin C-S, et al. (2013) Nonhybrid, finished microbial genome assemblies from long-read SMRT sequencing data. *Nat Methods* 10(6):563–569.
87. Sherwood R, Hagedorn DJ (1958) *Determining Common Root Rot Potential of Pea Fields* (Agricultural Experiment Station, University of Wisconsin, Madison, WI).
88. Jovel J, et al. (2016) Characterization of the gut microbiome using 16S or shotgun metagenomics. *Front Microbiol* 7:459.